A numerical study of Two-Dimensional Magnetized Bioconvective Unsteady fluid flow in two Stretching Parallel Plates with Internal Heating and Chemical Reaction Effects

Waris Khan[1,*], Haroon Ur Rasheed[2]

[1]Department of Mathematics & Statistics, Hazara University Mansehra, 21120 KP, Pakistan

[2]Department of Computer Science, Sarhad University of Science and Information Technology Peshawar, 25000 KP, Pakistan

Corresponding: wariskhan758@yahoo.com

Abstract: Driven by scientific development, the bio-convection unsteady nanofluid flow has gained enormous attention in research due to its applications in various disciplines such as biosensors, biological polymer synthesis, pharmaceutics, microbial improved oil recovery, and environment-friendly applications. As such, this study aims to investigate the mixed bio-convective magnetized and electrically conducting 2-dimensional flow in view of two extended wall channels subjected to MHD, thermal radiation, and binary chemical reaction effects. A mathematical framework is developed underflow of a nonofluid based on certain conditions. The implication of Soret and Dufour impacts is considered in the model problem. Such a nonlinear mathematical model is tackled by invoking similarity solutions for mass conservation, momentum, temperature, concentration, and micro-organisms expressions. The dimensionless principles (ODEs) are addressed by the efficacy Nactsheim-Swigert shooting along with the iteration process, explicitly through shooting technique (RK-4). The outlines of distinguished emerging constraints on flow fields are offered through the plotted graphic visuals. The impact of physical quantities of engineering interest is offered numerically via tabulated values.

1. Introduction

Numerous researchers, mathematicians, engineers, and scientists from several disciplines of science are currently interested in a variety of non-Newtonian fluids known as nano-liquids. Because of their widespread application in different manufacturing units which includes solar steam generation, electronic component freezing, aerospace tribology, and medical suspension sterilisation. According to Pal and Mondal [1], bio-convection improves the stability of the nanofluid flow. Kuznetsov and Avramenko [2] investigated bio-convection in fluid flow with gyrotactic bacteria and nano-size particles. Khan et al. [3] examined the boundary layer nanofluid flow of microorganisms with Naiver slip condition through a vertical channel. The impact of the gyrotactic microbe density factor on bio-convection flow over a stretching surface was studied by Tham et al. [4]. The fully developed flow of nanofluid in a horizontally flat conduit containing gyrotactic bacteria and nanoparticles was studied by Xu et al. [5]. Raees et al. [6] reported an unstable bio convective flow of Newtonian fluid including nanoparticles between two extended plate channels. Fluid flow in a horizontal channel with gyrotactic microorganisms, including nanoparticles, was explored by Mosayebidorcheh et al. [7]. Shen et al. [8] employed

HAM to explore bio-convective nanofluid flow with radiation and velocity slip effects moving motile microorganisms across a stretched surface. The analytical approach assisted Nagaraju et al. [9] in exploring the flow in a cylinder projected vertically under the influence of heat source/sink effects uniformly. Semi analytic solutions were obtained by Yusuf and Gambo [10] while studying the free convective flood of an incompressible liquid including heat source or sink properties over a cylinder with a porous material placed vertically. Dawar et al. [11] noticed attractive results on the stream of viscoelastic and Newtonian liquid with heat generation/absorption. Under the idea of a small Reynolds number and applying Debye-Huckel approximations over the energy and momentum equation, the solution is obtained by Shaheen et al. [12]. Thumma and Mishra [13] worked analytically using the Adomian decomposition method over the Eyring- Powell nanofluid flow over a sheet that is stretched. Temperature and heat sink/source effects were discussed in detail. Cu-water nanofluid is covered in a squared cavity and partial slip effect along the horizontal walls. Shukla et al. [14] investigated heat transfer in bioconvective nanofluid flow under the influence of solar flux, radiation, and oblique magnetic fields. Cheng [15] used the Soret and Dufour effects on a saturated fluid flow in a porous medium to explain natural convection. Hayat et al. [16] investigated the impact of Soret and Dufour on viscoelastic fluid flow through a porous surface in the presence of a magnetic field. Hayat et al. [17] examined hydromagnetic properties in the 3D flow of couple stress nano liquid. Numerical treatment for mixed convective nanoliquid flow in a lid-driven square cavity with three triangular heating blocks is reported by Boulahia et al. [18]. Hayat et al. [19] discussed the impact of the hydromagnetic 3D flow of nanoliquid induced by a nonlinear actuating sheet with the convective condition. Nanomaterial transport impact on hydromagnetic mixed convective nanofluids flow in micro-annuli with temperature-dependent thermophysical features is scrutinized by Malvandi et al. [20]. Hayat et al. [21] elaborated Darcy-Forchheimer 3D flow of Williamson nanofluid over a convectively heated nonlinearly moving surface. Numerical treatment for Magnetohydrodynamic three-dimensional radiative slip flow of nanofluids induced by a nonlinear accelerating surface is performed by Mahanthesh et al. [22]. Liu et al. [23] used lattice Boltzmann theory to create a dual-diffusion natural convective flow based on multi-relaxation phenomena with Soret and Dufour effects. They showed how to leverage the Soret and Dufour influences to create double-diffuse natural convection flow. In a Carreau fluid flow with Soret and Dufour effects, Sardar et al. [24] examined mixed convection processes. Bilal Ashraf et al. [25] addressed the mixed convective MHD viscoelastic fluid flow with Soret and Dufour impacts. Jiang et al. [26] have good results in simultaneous heat and mass transmission processes with Soret and Dufour effects. Hafeez et al. [27] investigated fluid flow across a disc exhibiting thermophoresis, Soret, and Dufour effects. Hannes Alfven was the first to invent and introduce magneto hydrodynamics in 1970. Drug targeting, astrophysics, MHD pumps, metallurgy, ship propulsion, turbulent drag reduction, and fusion reactors are examples of MHD uses in health sciences and engineering. The aforementioned utilizations of MHD motivate scientists to develop novel models in the field of fluid dynamics [28–31]. MHD flow across a variety of geometries relevant to engineering is a fascinating and worthwhile subject of research. Patel and Singh [32] investigated MHD, micropolar fluid flow with Brownian diffusion, and the convective boundary condition. A steady MHD hybrid nanofluid flow was examined by Aly and Pop [33] over a permeable flat plate. Rashid et al. [34] investigated the effects of radiation on the MHD boundary layer flow over a porous shrinking sheet. Waini et al. [35] explored magnetic field interactions with steady fluid flow through a permeable wedge. Sheikhpour et al. [36] analyzed nanofluids usage in biomedical, imaging, drug delivery as well as anti-bacterial fields. In recent years, transmission in porous media is an interesting incident, so it was utilized by Khanafer and Vafai [37] for investigation of uses regarding nanofluids. Heat transfer, as well as flow features of nanofluid flow having forced and free convection, was reviewed by Wang and Mujumdar [38].

2. Mathematical Formulation

Assuming an unsteady hydro-magnetic and electrically conducting bio-convective 2D flow of nanofluid between two extended plates channel subject to first order binary reaction, and the impact of Dufour and Soret are considered in modeling the flow problem. Figure 1 portrays the geometry and coordinate system selected in such a way that the $x-$direction is taken in the direction of the lower plate and $y-$axis normal to flow. The magnetic field is assumed in the normal direction. The plates are at $y = h\left(\bar{t}\right) = \left(\upsilon\left(1-at\right)/b\right)^{0.5}$ distance apart, and the upper plate is move away from the lower plate with $\bar{v}\left(\bar{t}\right) = dh/d\bar{t}$. Where, $\bar{t}$ is time, υ kinetic viscosity, and a, b are constants. Moreover, $1-at \geq 0$ shows that $\sqrt{b^2-4ac}\,1/t > 0$. Obviously, $a = 0$ designates plates are stationary, $0 < a < 1/t$ show that upper plate is squeezed against the lower one, and $a < 0$ show that the upper plate is move away from the lower plate. It is considered that both walls are preserved at a constant binary reaction concentration C_1 *and* C_2, constant temperatures T_1 , T_2 and constant microorganisms N_1 *and* N_2.

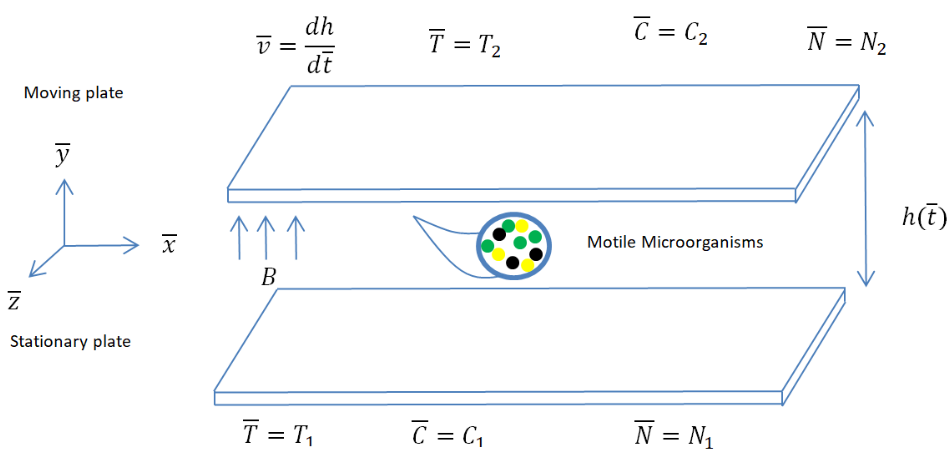

Fig. 1 Flow configuration of the problem

The constitutive flow system under specified assumptions is as follows:

$$\nabla \cdot \overline{V} = 0 \tag{1}$$

$$\frac{\partial \overline{V}}{\partial \bar{t}} + \left(\nabla \cdot \overline{V}\right)\overline{V} = \upsilon \nabla^2 \overline{V} + \frac{1}{\rho}\left(J \times B\right) - \frac{1}{\rho}\nabla p \tag{2}$$

$$\frac{\partial \overline{T}}{\partial \bar{t}} + \overline{V} \cdot \nabla \overline{T} = \alpha \nabla^2 \overline{T} + \frac{Q_s\left(\bar{t}\right)}{\rho c_p}\left(\overline{T} - \overline{T}_0\right) + J \tag{3}$$

$$\frac{\partial \overline{C}}{\partial \bar{t}} + \overline{V} \cdot \nabla \overline{C} = D \nabla^2 \overline{C} + k\left(\bar{t}\right)\left(\overline{C} - \overline{C}_0\right) + R \tag{4}$$

$$\frac{\partial \overline{N}}{\partial \bar{t}} = -\nabla \cdot j \tag{5}$$

Where $B,\ J,\ \overline{V},\ p,\ \rho,\ \upsilon,\ \alpha,\ \overline{T},\ \overline{T}_0,\ D,\ \overline{C},\ \overline{C}_0\ , Q_s\left(\bar{t}\right),\ \overline{N},\ K\left(\bar{t}\right)\ and\ j$ are magnetic field, electric current density, velocity vector, pressure, fluid density, kinematic viscosity, thermal diffusivity, temperature, reference temperature, mass diffusivity, concentration, reference concentration, volumetric heat generation rate, motile microorganism, chemical reaction, and heat flux. Herein $j = \rho D K_t / C_s \nabla^2 \overline{C}$ is the Dufour effect given by Frick's law, R is the flux concentration due to the temperature difference known as Soret effect from Fourier's law, $R_c = q/A = D K_t / T_m \nabla^2 \overline{T}$, $K_t,\ D,\ and\ T_m$ is the thermal diffusion ratio, coefficient of diffusion, and mean temperature.

The respective component form of Eq. (2) for 2-dimenssional fluid flow may be expressed as:

$$\frac{\partial \bar{u}}{\partial \bar{t}} + \bar{u}\frac{\partial \bar{u}}{\partial \bar{x}} + \bar{v}\frac{\partial \bar{u}}{\partial \bar{y}} = \frac{1}{\rho}\frac{\partial p}{\partial \bar{x}} + \upsilon\left(\frac{\partial^2 \bar{u}}{\partial \bar{x}^2} + \bar{u}\frac{\partial^2 \bar{u}}{\partial \bar{y}^2}\right) - \frac{\sigma}{\rho}B^2\left(t\right)\bar{u} \tag{6}$$

$$\frac{\partial \bar{v}}{\partial \bar{t}} + \bar{u}\frac{\partial \bar{v}}{\partial \bar{x}} + \bar{v}\frac{\partial \bar{v}}{\partial \bar{y}} = -\frac{1}{\rho}\frac{\partial p}{\partial \bar{y}} + \upsilon\left(\frac{\partial^2 \bar{v}}{\partial \bar{x}^2} + \bar{u}\frac{\partial^2 \bar{v}}{\partial \bar{y}^2}\right) \tag{7}$$

By simplifying Eqs. (6) and (7), the following transformation is used given in Eq. (8):

$$\varsigma = \frac{\partial \bar{v}}{\partial \bar{x}} - \frac{\partial \bar{u}}{\partial \bar{y}} = -\nabla \xi \tag{8}$$

In view of the above assumptions the resulting equations may be expressed as:

Mass conservation relation

$$\frac{\partial \bar{u}}{\partial \bar{x}}+\frac{\partial \bar{v}}{\partial \bar{y}}=0 \tag{9}$$

Momentum expression

$$\frac{\partial \varsigma}{\partial \bar{t}}+\bar{u}\frac{\partial \varsigma}{\partial \bar{x}}+\bar{v}\frac{\partial \varsigma}{\partial \bar{y}}=\upsilon\left(\frac{\partial^2 \varsigma}{\partial \bar{x}^2}+\bar{u}\frac{\partial^2 \varsigma}{\partial \bar{y}^2}\right)-\frac{\sigma}{\rho}B^2(t)\frac{\partial \bar{u}}{\partial \bar{y}} \tag{10}$$

Energy appearance

$$\frac{\partial \bar{T}}{\partial \bar{t}}+\bar{u}\frac{\partial \bar{T}}{\partial \bar{x}}+\bar{v}\frac{\partial \bar{T}}{\partial \bar{y}}=\frac{k}{\rho c_p}\left(\frac{\partial^2 \bar{T}}{\partial \bar{x}^2}+\frac{\partial^2 \bar{T}}{\partial \bar{y}^2}\right)+\frac{1}{\rho c_p}Q_s(t)\left(\bar{T}-\bar{T}_0\right)+\frac{Dk_t}{c_s c_p}\left(\frac{\partial^2 \bar{C}}{\partial \bar{x}^2}+\frac{\partial^2 C}{\partial \bar{y}^2}\right) \tag{11}$$

Concentration equation

$$\frac{\partial \bar{C}}{\partial \bar{t}}+\bar{u}\frac{\partial \bar{C}}{\partial \bar{x}}+\bar{v}\frac{\partial \bar{C}}{\partial \bar{y}}=D\left(\frac{\partial^2 \bar{C}}{\partial \bar{x}^2}+\frac{\partial^2 \bar{C}}{\partial \bar{y}^2}\right)+K(t)\left(\bar{C}-\bar{C}_0\right)+\frac{Dk_t}{\bar{T}_m}\left(\frac{\partial^2 \bar{T}}{\partial \bar{x}^2}+\frac{\partial^2 T}{\partial \bar{y}^2}\right) \tag{12}$$

Motile gyrotactic microorganisms

$$\frac{\partial \bar{N}}{\partial \bar{t}}+\frac{\partial \bar{N}\tilde{v}}{\partial \bar{x}}+\frac{\partial \bar{N}\tilde{v}}{\partial \bar{y}}+\bar{u}\frac{\partial \bar{N}}{\partial \bar{x}}+\bar{v}\frac{\partial \bar{N}}{\partial \bar{y}}=D_m\left(\frac{\partial^2 \bar{N}}{\partial \bar{x}^2}+\frac{\partial^2 \bar{N}}{\partial \bar{y}^2}\right) \tag{13}$$

Conditions are:

$$\begin{cases}\bar{y}=0: \ \bar{u}=0, \ \bar{v}=0, \ \bar{T}=T_1, \ \bar{C}=C_1, \bar{N}=N_1 \\ \bar{y}=h(\bar{t}): \ \bar{u}=0, \ \bar{v}=\dfrac{dh}{d\bar{t}}, \ \bar{T}=T_2, \ \bar{C}=C_2, \ \bar{N}=N_2\end{cases} \tag{14}$$

where $\bar{u}=\frac{\partial \xi}{\partial \bar{y}}$ and $\bar{v}=-\frac{\partial \xi}{\partial \bar{x}}$ are velocity factors, $\varsigma=-\nabla^2\xi$ is the vorticity function, $\bar{N}$ is the microorganisms density, W_c is the cell moment, $\tilde{v}=b_c W_c \big/ \left(C_1-\bar{C}_0\right)\partial \bar{C}/\partial \bar{y}$ denote the microorganisms average velocity, b_c constant, and D_m diffusivity of microorganisms.

Following similarity variables are suggested:

$$\xi\left(\bar{x},\bar{y}\right)=\left(\frac{b\upsilon}{1-a\bar{t}}\right)^{\frac{1}{2}}xF\left(\chi\right),\ \bar{u}=\frac{bx}{1-a\bar{t}}F^{'}\left(\chi\right),\ \bar{v}=-\left(\frac{b\upsilon}{1-a\bar{t}}\right)^{\frac{1}{2}}F\left(\chi\right),\ \chi=\left(\frac{b}{\upsilon\left(1-a\bar{t}\right)}\right)^{\frac{1}{2}}\bar{y},$$
$$T\left(\chi\right)=\frac{\bar{T}-\bar{T}_0}{T_1-\bar{T}_0},\ C\left(\chi\right)=\frac{\bar{C}-\bar{C}_0}{C_1-\bar{C}_0},\ w\left(\chi\right)=\frac{\bar{N}}{N_1} \tag{15}$$

One gets the resulting nonlinear couples system of equations with aid of Eq. (15) in Eqs. (9)–(12) in the dimensionless form as:

$$F^{''''}-MF^{''}-\beta\chi F^{'''}-3\beta F^{'}-F^{''}F^{'}+F^{'''}F=0 \tag{16}$$

$$T^{''}+\Pr\left(QT-\beta\chi T^{'}+FT^{'}+D_fC^{'}\right)=0 \tag{17}$$

$$C^{''}-Sc\left(KrC-\beta\chi C^{'}+FC^{'}+SrT^{''}\right)=0 \tag{18}$$

$$w^{''}-Sc\left(\beta\chi w^{'}-Fw^{'}\right)-Pe\left(\chi C^{''}+C^{'}w^{'}\right)=0 \tag{19}$$

with extremes conditions:

$$\begin{cases}\chi=0:\ F=0,\ F^{'}=0,\ T=1,\ C=1,w=1\\ \chi=1:\ F=\beta,\ F^{'}=0,\ T=\delta_T,\ C=\delta_C\ ,w=\delta_w\end{cases} \tag{20}$$

Here, the symbols/parameters

$$\beta=\frac{2}{2b},\ M=\frac{\sigma}{\upsilon\rho B_0^2},\ \Pr=\frac{\rho C_p\upsilon}{k},\ Df=\frac{Dk_{\bar{T}}\left(C_1-\bar{C}_0\right)}{\upsilon C_p\left(T_1-\bar{T}_0\right)},\ Q=\frac{Q_0}{\rho C_p},St=\frac{Dk_{\bar{T}}\left(T_1-\bar{T}_0\right)}{\upsilon\bar{T}_m\left(C_1-\bar{C}_0\right)},$$

$$Le=\frac{\alpha}{D},Sc=\frac{\upsilon}{D},\ Kr=\left(b/1-at\right)^{-1}k\left(\bar{t}\right)\ and\ Pe\ whereas\ \delta_T=T_2-\bar{T}_0/T_1-\bar{T}_0,$$
$$\delta_C=C_2-\bar{C}_0/C_1-\bar{C}_0,\ \delta_w=N_2/N_1$$

Labeled as squeezing parameter, magnetic field, Dufour number, heat generation parameter, Soret number, Lewis number, Schmidt number, chemical reaction parameter, and bio convection Peclet number respectively, whereas $\delta_T,\ \delta_C,\ \delta_w$ are constants. The magnetic field strength and internal heating is defined as $B_0=\left(b/\upsilon\left(1-at\right)\right)^{\frac{-3}{4}}B\left(\bar{t}\right)\ and\ Q_0=\left(b/1-at\right)^{-1}Q_s\left(\bar{t}\right)$.

3. Solution methodology

There are numerous methods for addressing nonlinear problems. Solving analytically these types of equations are so tedious due to nature complexity. Thus an efficient and validated numerical algorithm through shooting method references [39-42]. Because of its rapid convergence, it is preferred over many other analytical and numerical approaches. The RK-4 method is intrinsically stable and convergent. In general, this technique has been employed for the BVP because of their exceptionally good stability qualities and fourth-order precision. The iterative procedure is continued until the required results are achieved to meet the convergence requirement up to accuracy point 10^{-6} by taking the step size is 0.01. The preliminary stage needs to shift all the ODEs Eqs. (7)- (10) into first order ODEs. For the convenience of the reader the flow path of the computational framework shown in Fig. 2.

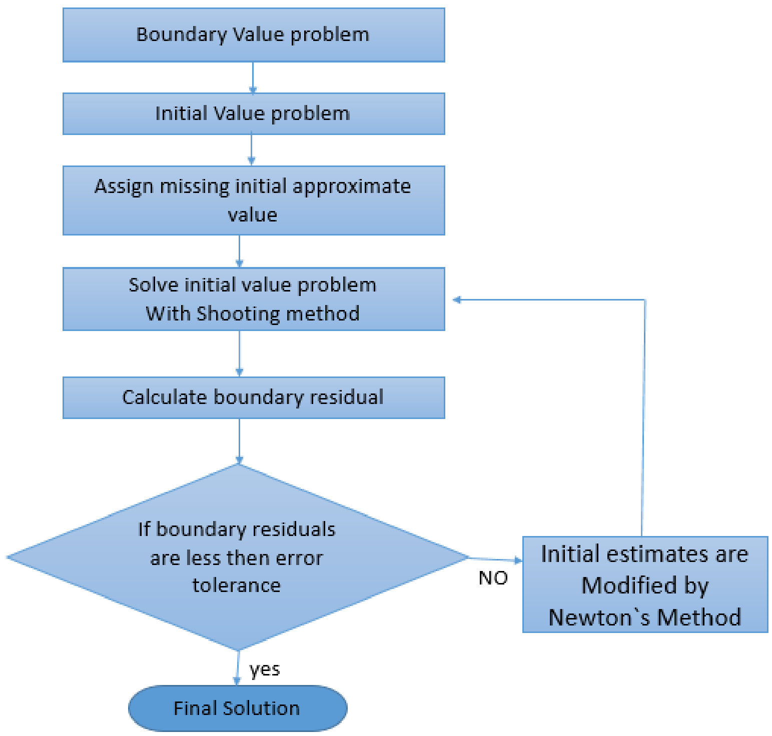

Fig. 2 Continued

3.1 Verification of Code

The correctness of the numerical method is measured by comparison the numerical outcomes on velocity, temperature and nanofluid-concentration from the analytical approach against the current consequences obtained and summarizes the comparison of analytic (HAM) and numerical solution is presented through plotted graphs Fig.3 and tabulated values given in table 1.

Fig. 3(a–d) Graphical comparisons of $F'(\chi), T(\chi), C(\chi)$ *and* $w(\chi)$ functions

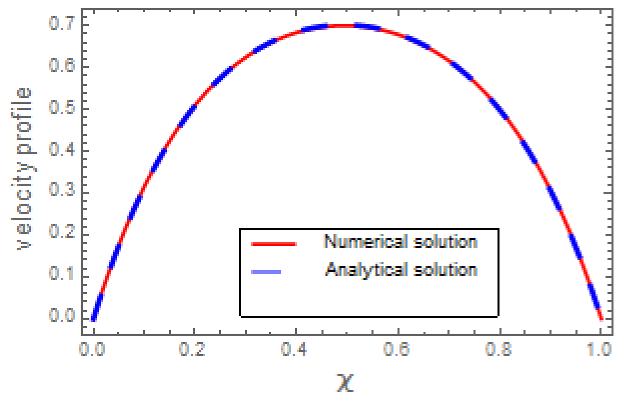

(a)

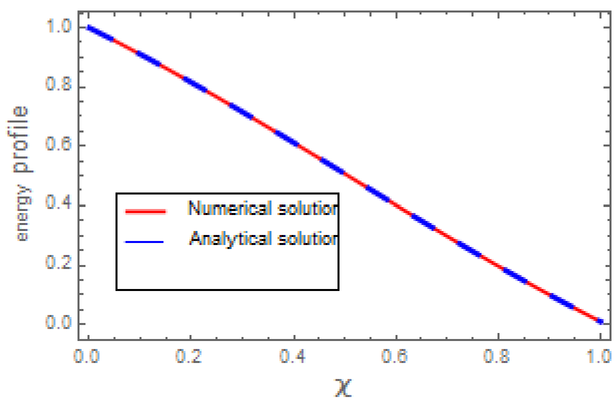

(b)

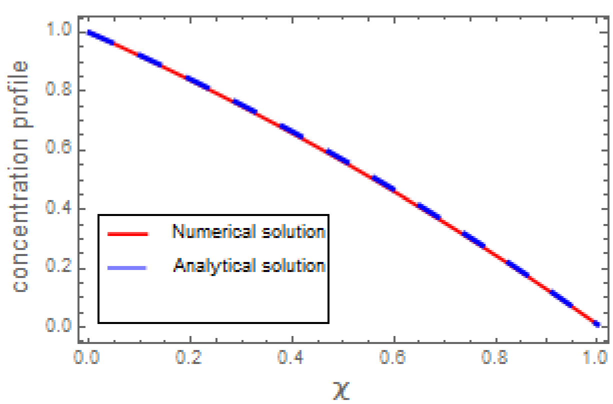

(c)

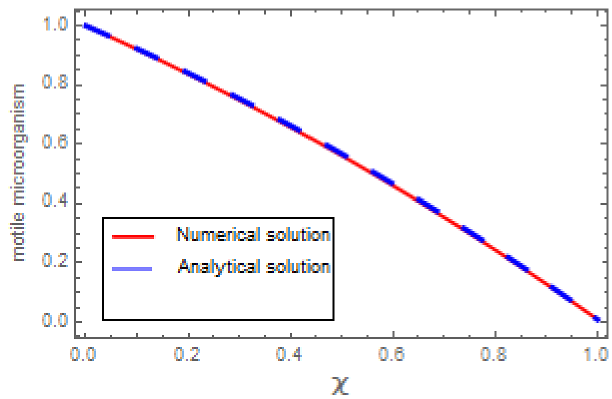

(d)

Table 1(a–d) Numerical comparison for velocity, energy, concentration, and motile microorganism

η	HAM solution	Numerical soltuion	Absolute Error
0.	-2.71051×10^{-20}	0.000000	2.7105×10^{-20}
0.1	0.315400	0.313749	0.001651
0.2	0.510029	0.509174	0.000855
0.3	0.624514	0.625047	0.000533
0.4	0.683397	0.685000	0.001602
0.5	0.699910	0.701867	0.001957
0.6	0.678548	0.680047	0.001500
0.7	0.615914	0.616275	0.000361
0.8	0.499986	0.498950	0.001035
0.9	0.307648	0.305879	0.001769
1.0	5.8102×10^{-8}	4.8261×10^{-8}	9.84119×10^{-9}

(a)

η	HAM solution	Numerical soltuion	Absolute Erro
0.	1.000000	1.000000	0.000000
0.1	0.910434	0.910728	0.000295
0.2	0.815189	0.815606	0.000417
0.3	0.715304	0.715698	0.000394
0.4	0.612101	0.612366	0.000266
0.5	0.507096	0.507175	0.000079
0.6	0.401903	0.401789	0.000114
0.7	0.298147	0.297884	0.000263
0.8	0.197370	0.197052	0.000318
0.9	0.100949	0.100708	0.000240
1.0	0.010000	0.010000	3.588050×10^{-11}

(b)

η	HAM solution	Numerical soltuion	Absolute Error
0.0	1.000000	1.000000	0.000000
0.1	0.920602	0.922540	0.001938
0.2	0.837148	0.840714	0.003566
0.3	0.749489	0.754331	0.004842
0.4	0.657506	0.663230	0.005724
0.5	0.561103	0.567267	0.006164
0.6	0.460198	0.466313	0.006115
0.7	0.354719	0.360245	0.005526
0.8	0.244591	0.248938	0.004347
0.9	0.129726	0.132249	0.002524
1.0	0.010000	0.010000	1.6405×10^{-10}

(c)

η	HAM solution	Numerical soltuion	Absolute Error
0.0	1.000000	1.000000	0.000000
0.1	0.920602	0.920797	0.000195
0.2	0.837148	0.837507	0.000359
0.3	0.749489	0.749975	0.000486
0.4	0.657506	0.658080	0.000574
0.5	0.561103	0.561720	0.000617
0.6	0.460198	0.460809	0.000611
0.7	0.354719	0.355270	0.000552
0.8	0.244591	0.245024	0.000433
0.9	0.129726	0.129977	0.000251
1.0	0.010000	0.010000	1.61663×10^{-11}

(d)

4. Consequences and discussion

In this section, the numerical solutions of coupled ordinary differential Eqs. (16) − (19) with boundary conditions Eq. (20) are obtained through shooting Fehlberg method. Our central concern is to debate the variation of the parameters such as squeezing parameter β, dimensionless magnetic field M, heat generation parameter Q, Dufour number Df, Soret number Sr, Schmidt number Sc, chemical reaction parameter K_0, and Peclet number Pe on velocity, energy, concentration, and motile microorganism outlines is presented in Figures 3–16.

From Figure 3, the outlines of M on the $F'(\chi)$ profile. It is observed that fluid velocity $F'(\chi)$ improves quickly with the higher estimation of magnetic parameter, whereas an increase in M values enhances $F'(\chi)$ in the vicinities of upper and lower plates, yields decay in $F'(\chi)$ profile between the plates. Physically, larger magnetic parameter interacts with electrically conductive nanofluid which drags of fluid flow due to Lorentz force. In consequences fluid velocity $F'(\varsigma)$

profile is diminished. Figure 4 displays the effect of squeezing parameter β on $F^{'}(\chi)$ outlines. It can be interpreted that velocity profile enhances with the increasing values of the β. This is due to the fact that the accelerated fluid has a greater velocity $F^{'}(\chi)$. Figure 5 unveils the outcome of heat generation parameter Q on thermal field profile $T(\chi)$. It can be observed that $T(\chi)$ rises through the growing values of Q parameter. Physically, higher estimation of Q increase the internal energy due to which the kinetic energy of the nanofluid particles increases yields an increment in the thermal boundary layer as well the in the thermal field. Figure 6 designates the result of the binary reaction parameter Kr on energy $T(\chi)$ field. It can be perceived that thermal field curve develops with the growing values of Kr parameter. Attributes of Dufour number Df on energy field curves $T(\chi)$ is outlines in Figure 7. It can be witnessed from plot that the energy field is strengthened with the increasing values of Dufour number. An increment in Df number yields to enhance the concentration. Inconsequence a rapid diffusion in is happened, due to which energy transfer increases in nanoparticles. Consequently, $T(\chi)$ profile increases. Figure 8 discloses the influence of Soret number St on temperature curves $T(\chi)$. As noticed that the incrementing values of St number develops the energy field curves $T(\chi)$. Figure 9 describes the effect of heat generation parameter Q on concentration $C(\chi)$ profile. It is clear from this plot that both $C(\chi)$ profile and the associated boundary layer thickness are diminishing subject to higher estimation of the heat generation parameter Q. Figure 10 explains the upshot of the binary reaction parameter Kr upon $C(\chi)$ outlines. It can be observed that the changing values of Kr decreasing the concentration profile as well as the concentration boundary layer. Physically, this decrease in $C(\chi)$ is because of the decline in molecular diffusivity with larger chemical species. Figure 11 outlines behavior of Dufour number Df on $C(\chi)$. It can be clearly witnessed that concentration profiles dwindles with the expanding values of Df number. Figure 12 explains the result of Soret number St on $C(\chi)$ profile; as noticed that larger estimation of number St declining the concentration profile. Figure 13 describes Sc upshot against $C(\chi)$. Physically, Sc and D are inversely related with each other. Hence, an augmentation in Sc values reasons decay in the $C(\chi)$ profile. Physically, D declines when Sc number increases. Thus $C(\chi)$ diminishes for expanding values of Sc. Figures 14–16 elucidated the consequences of Soret number St and Dufour number Df on microorganism's $w(\chi)$ profile. One can observed a decline trends in $w(\chi)$ profile for expanding values of both Soret and Dufour numbers is observed in these plots. A greater St and Df optimum reduces the density of motile microorganism $w(\chi)$ profile shown in Figure 14 and 15. Figure 16 explained that the pattern for Peclet number Pe against motile microorganism $w(\chi)$ profile. The increasing values of Pe parameter there is a decreasing behavior in $w(\chi)$ profile. The empirical impacts of this propensity are related to a decay in motile-diffusivity due to which a loss in $w(\chi)$ as well as in decline in the density of microorganism.

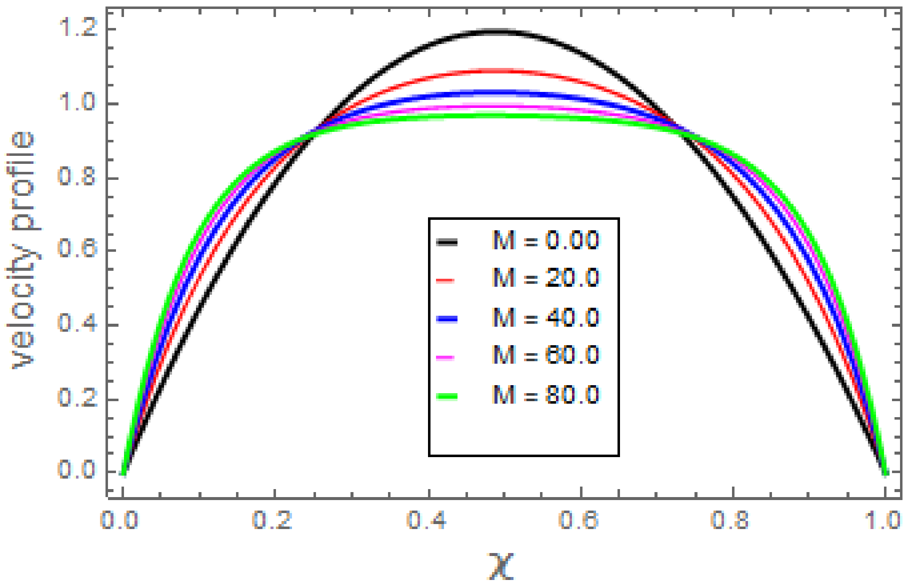

Fig. 3 Result of M against $F^{'}(\chi)$

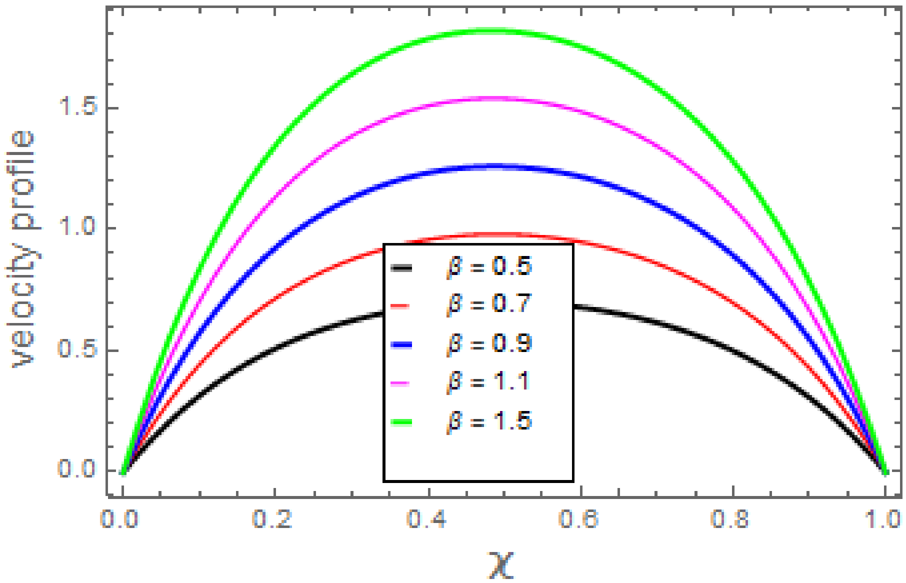

Fig. 4 Result of β against $F^{'}(\chi)$

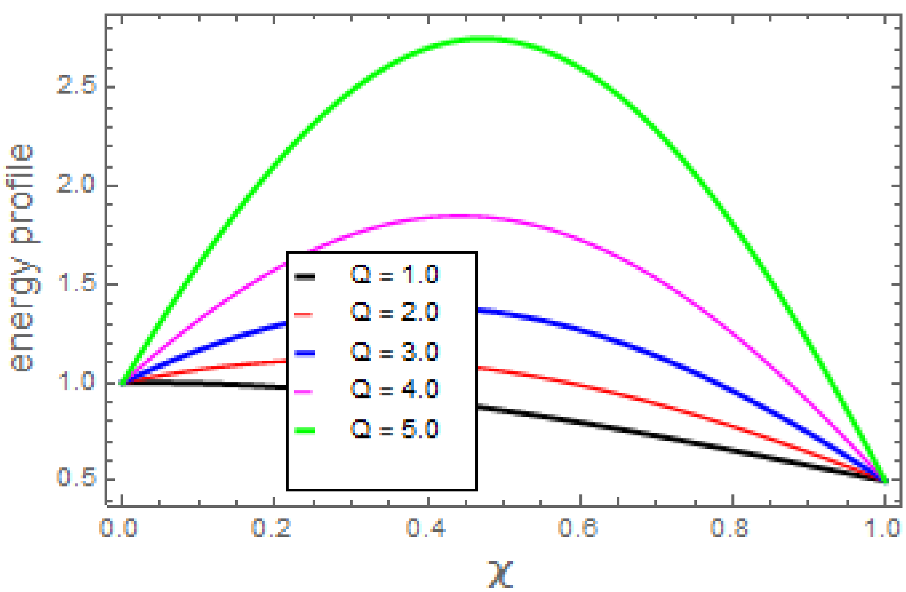

Fig. 5 Result of Q against $T(\chi)$

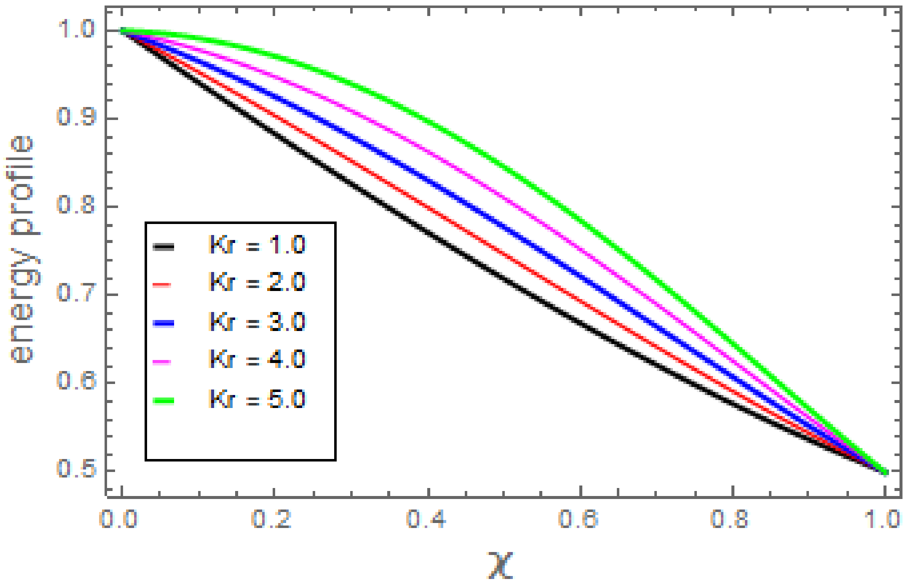

Fig. 6 Result of Kr against $T(\chi)$

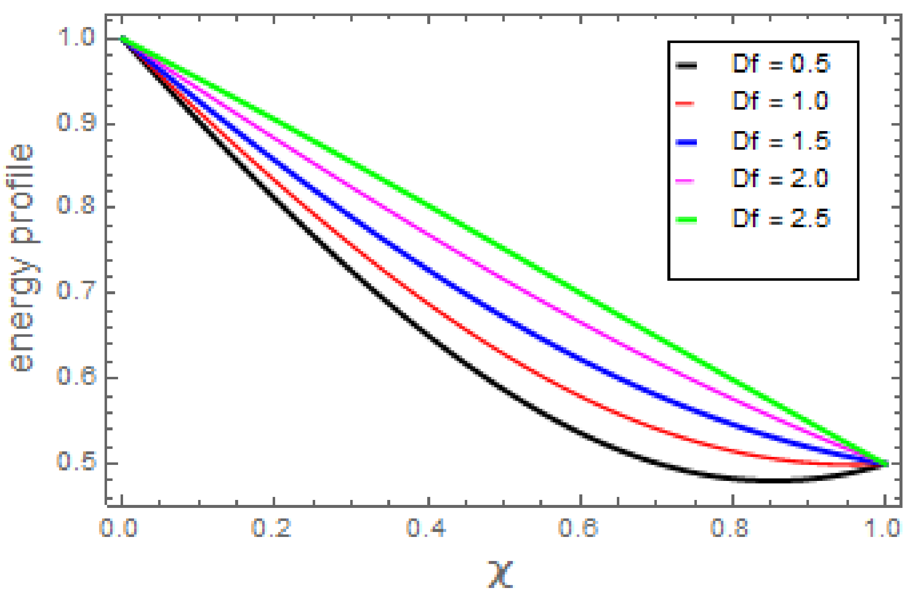

Fig. 7 Result of Df against $T(\chi)$

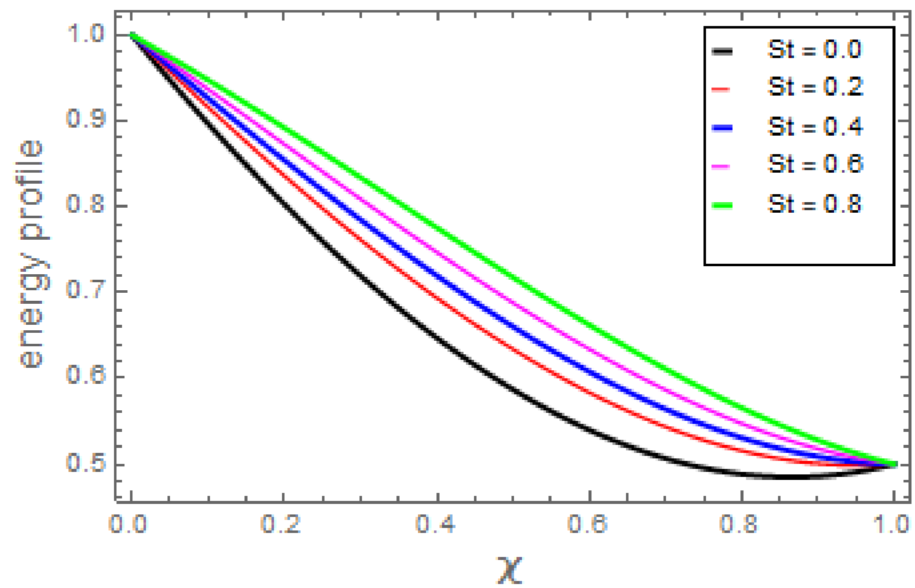

Fig. 8 Result of St against $T(\chi)$

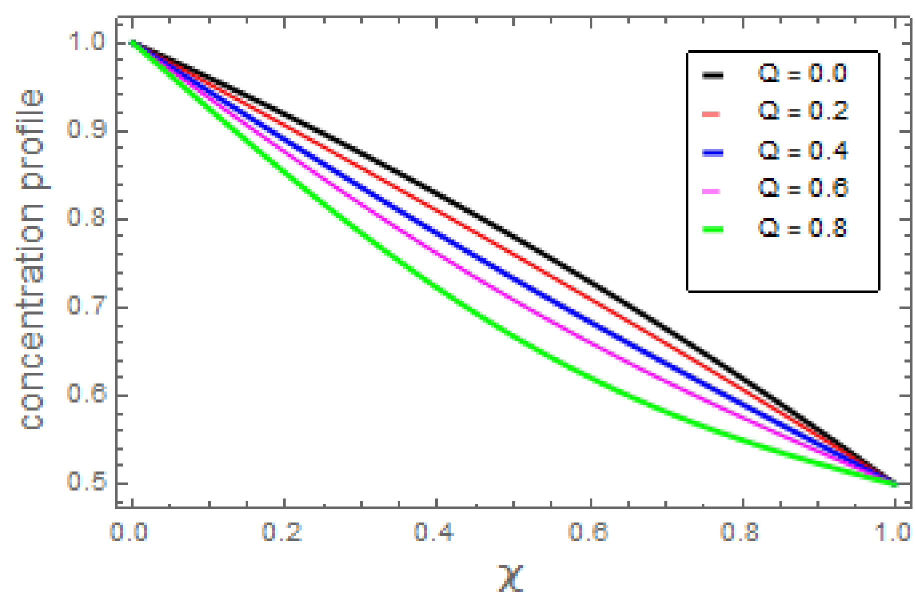

Fig. 9 Result of Q against $C(\chi)$

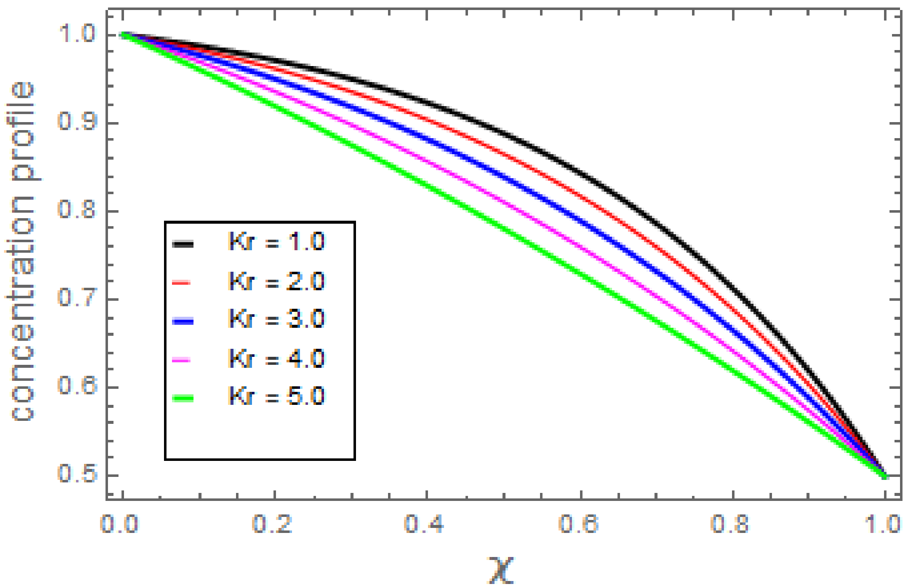

Fig. 10 Result of Kr against $C(\chi)$

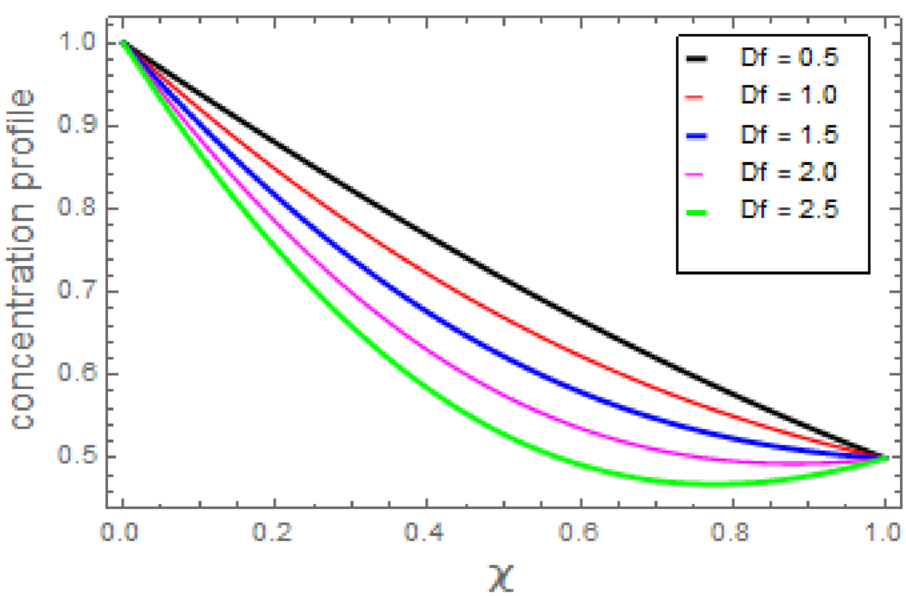

Fig. 11 Result of Df against $C(\chi)$

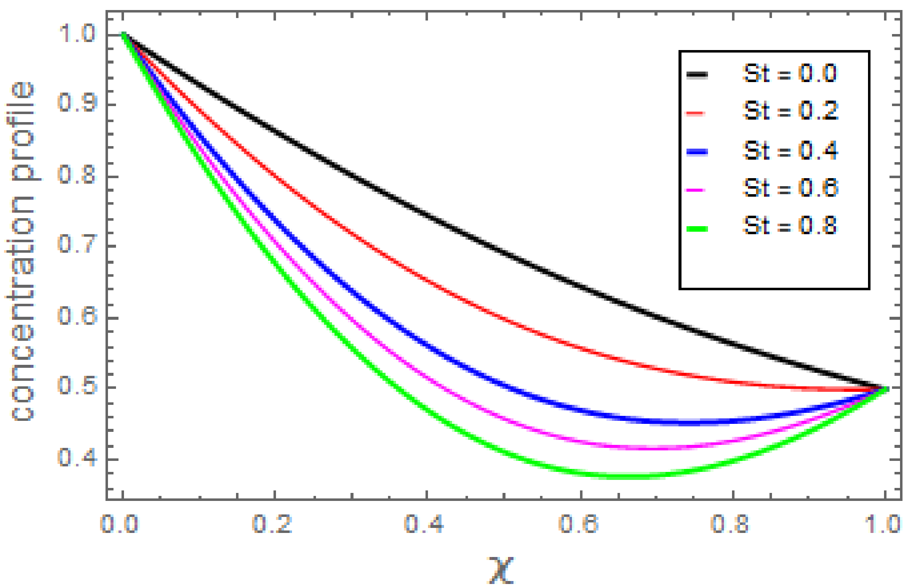

Fig. 12 Result of St against $C(\chi)$

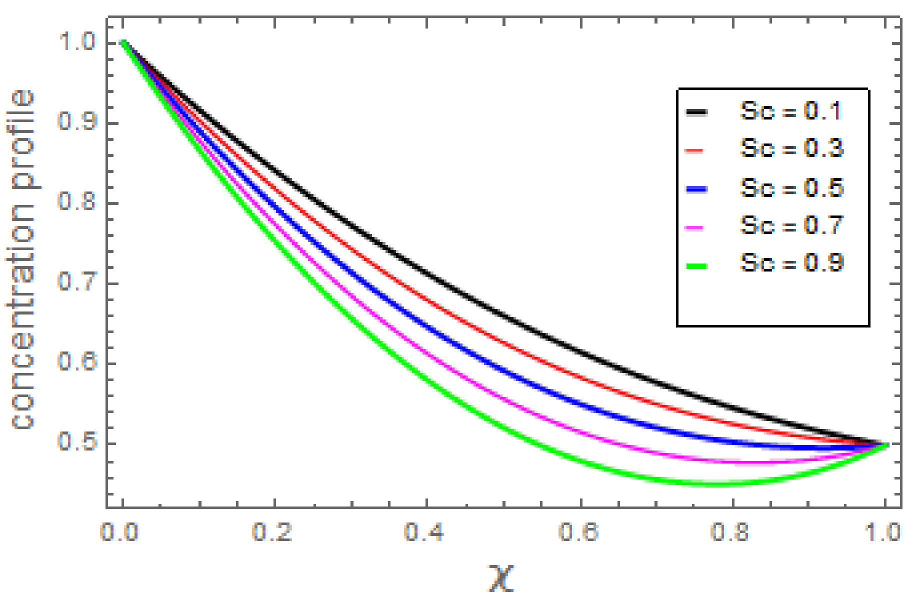

Fig. 13 Result of Sc against $C(\chi)$

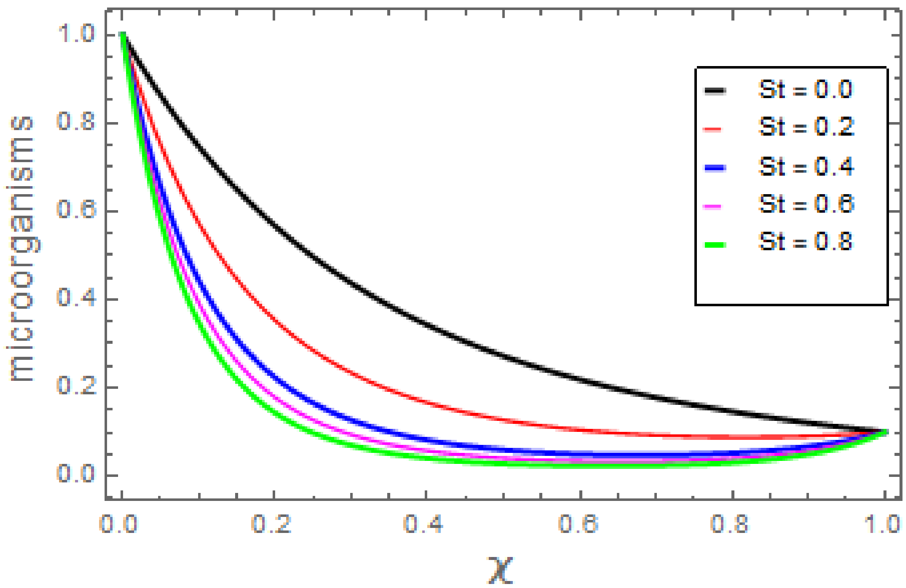

Fig. 14 Result of St against $w(\chi)$

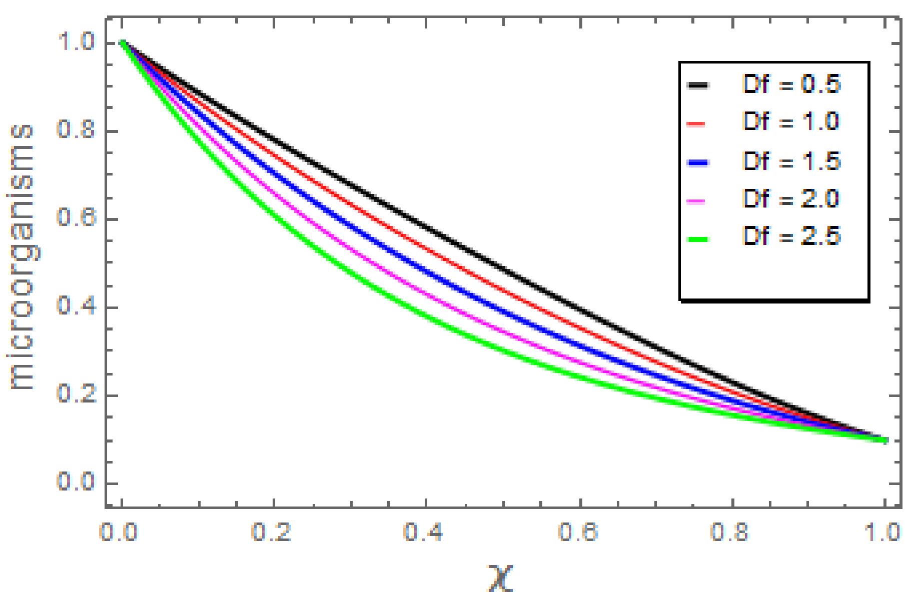

Fig. 15 Result of Df against $w(\chi)$

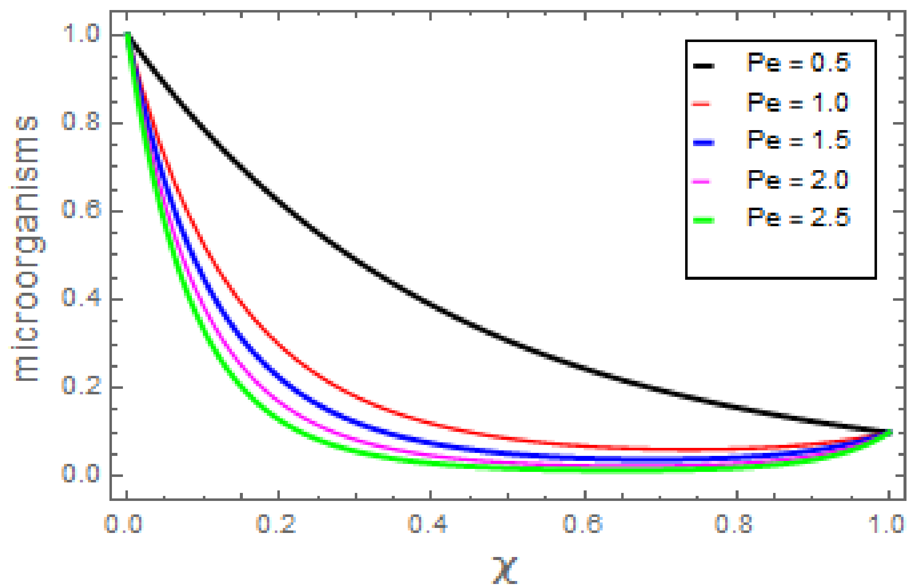

Fig. 16 Result of Pe against $w(\chi)$

5. Conclusions

The present model explores the role of Soret and Dufour effects in unsteady bio-convective electrically conducting nanofluid between two parallel plates channel containing motile microorganismin a horizontal channel. The model problem described a nonlinear coupled system of ODEs are tackled for numerical solution through an efficient and validated numerical algorithm via shooting technique. The specific outcomes of this study are listed:

- It has been observed that velocity outline is decreased in the middle and increases partially with the parallel walls.
- The expanding squeezing parameter values diminishing the fluid flow significantly within the flow domain.
- An increment in binary reaction parameter, heat generation, and Dufour and Soret constraints developed the thermal field curves.
- The increase in the chemical reaction parameter caused in decline in both concentration and motile microorganism.
- For higher estimation of the Schmidth number, heat generation, and Dufour and Soret parameters increases the concentration profile significantly.
- Motile microorganism curves are dwindled subject to higher values of Dufour and Soret numbers and Peclet number.
- For growing values of Peclet number decline the density of motile microorganism.

Funding: Authors will pay all the outstanding dues after the acceptance of this manuscript.
Data Availability Statement: The data used to support the findings of this study are available from the corresponding author upon request.
Conflicts of Interest: The authors declare no conflict of interest.

References

1. D. Pal and S. K. Mondal, "MHD nanofluid bioconvection over an exponentially stretching sheet in the presence of gyrotactic microorganisms and thermal radiation," BioNanoScience, vol. 8, no. 1, pp. 272–287, 2018.
2. A. V. Kuznetsov and A. A. Avramenko, "Effect of small particles on this stability of bioconvection in a suspension of gyrotactic microorganisms in a layer of finite depth," International Communications in Heat and Mass Transfer, vol. 31, no. 1, pp. 1–10, 2004.
3. W. A. Khan, O. D. Makinde, and Z. H. Khan, "MHD boundary layer flow of a nanofluid containing gyrotactic microorganisms past a vertical plate with Navier slip," International Journal of Heat and Mass Transfer, vol. 74, pp. 285–291, 2014.
4. L. .am, R. Nazar, and I. Pop, "Mixed convection flow over a solid sphere embedded in a porous medium filled by a nanofluid containing gyrotactic microorganisms," International Journal of Heat and Mass Transfer, vol. 62, pp. 647–660, 2013.
5. H. Xu and I. Pop, "Fully developed mixed convection flow in a horizontal channel filled by a nanofluid containing both nanoparticles and gyrotactic microorganisms," European Journal of Mechanics - B: Fluids, vol. 46, pp. 37–45, 2014.
6. A. Raees, H. Xu, and S.-J. Liao, "Unsteady mixed nanobioconvection flow in a horizontal channel with its upper plate expanding or contracting," International Journal of Heat and Mass Transfer, vol. 86, pp. 174–182, 2015.
7. S. Mosayebidorcheh, M. A. Tahavori, T. Mosayebidorcheh, and D. D. Ganji, "Analysis of nano-bioconvection flow containing both nanoparticles and gyrotactic microorganisms in a horizontal channel using modified least square method (MLSM)," Journal of Molecular Liquids, vol. 227, pp. 356–365, 2017.
8. B. Shen, L. Zheng, C. Zhang, and X. Zhang, "Bioconvection heat transfer of a nanofluid over a stretching sheet with Mathematical Problems in Engineering 13velocity slip and temperature jump," Eermal Science, vol. 21, no. 6, pp. 2347–2356, 2017.
9. G. Nagaraju, M. Garvandha, J.V.R. Murthy, MHD flow in a circular horizontal pipe under heat source/sink with suction/injection on wall, Front. Heat Mass Transf. 13(6) (2019) 1–8.
10. T.S. Yusuf, D. Gambo, Role of heat source/sink on time dependent free convective flow in a coaxial cylinder filled with porous material: A semi analytical approach, International Journal of Applied Power Engineering. 8(1) (2020) 67–77.
11. Dawar, Z. Shah, P. Kuman, H. Alrabaiah, W. Khan, S. Islam, N. Shaheen, Chemically reactive MHD micropolar nanofluid flow with velocity slips and variable heat source/sink, Sci. Rep. 10 (2020) 20926.

12. S. Shaheen, O.A. Bég, F. Gul, K. Maqbool, Electro-Osmotic propulsion of Jeffrey fluid in a ciliated channel under the effect of nonlinear radiation and heat source/sink, J. Biomech. Eng. 143(5) (2021) 051008.
13. T. Thumma, S.R. Mishra, Effect of nonuniform heat source/sink, and viscous and Joule dissipation on 3D Eyring–Powell nanofluid flow over a stretching sheet, J. Comput. Des. Eng. 7(4) (2020) 412–426.
14. N. Shukla, P. Rana, S. Kuharat, and O. A. Beg, "Non-similar radiative bioconvection nanofluid flow under oblique magnetic field with entropy generation," Journal of Applied and Computational Mechanics, vol. 8, no. 1, pp. 206–218, 2020.
15. C.-Y. Cheng, "Soret and Dufour effects on heat and mass transfer by natural convection from a vertical truncated cone in a fluid-saturated porous medium with variable wall temperature and concentration," International Communications in Heat and Mass Transfer, vol. 37, no. 8, pp. 1031–1035, 2010.
16. T. Hayat, M. Mustafa, and I. Pop, "Heat and mass transfer for Soret and Dufour's effect on mixed convection boundary layer flow over a stretching vertical surface in a porous medium filled with a viscoelastic fluid," Communications in Nonlinear Science and Numerical Simulation, vol. 15, no. 5, pp. 1183–1196, 2010.
17. T. Hayat, A. Aziz, T. Muhammad and B. Ahmed, Influence of magnetic field in three dimensional flow of couple stress nanofluid over a nonlinearly stretching surface with convective condition, Plos One, 10 (2015) e0145332.
18. Z. Boulahia, A. Wakif and R. Sehaqui, Numerical investigation of mixed convection heat transfer of nanofluid in a lid driven square cavity with three triangular heating blocks, Int. J. Comput. Appl., 143 (2016) 37-45.
19. T. Hayat, A. Aziz, T. Muhammad and A. Alsaedi, On magnetohydrodynamic three dimensional flow of nanofluid over a convectively heated nonlinear stretching surface, Int. J. Heat Mass Transfer, 100 (2016) 566-572.
20. Malvandi, S.A. Moshizi and D.D. Ganji, Nanoparticle transport effect on magnetohydrodynamic mixed convection of electrically conductive nanofluids in micro-annuli with temperature-dependent thermophysical properties, Physica E: Low-dim. Sys. Nanostruc., 88 (2017) 35-49.
21. T. Hayat, A. Aziz, T. Muhammad and A. Alsaedi, Darcy-Forchheimer three-dimensional flow of Williamson nanofluid over a convectively heated nonlinear stretching surface, Commun. Theor. Phys., 68 (2017) 387-394.
22. B. Mahanthesh, B.J. Gireesha, R.S.R. Gorla and O.D. Makinde, Magnetohydrodynamic three-dimensional flow of nanofluids with slip and thermal radiation over a nonlinear stretching sheet: a numerical study, Neural Comp. Appl., 30 (2018) 1557-1567.
23. Q. Liu, X.-B. Feng, X.-T. Xu, and Y.-L. He, "Multiple-relaxation-time lattice Boltzmann model for double-diffusive convection with Dufour and Soret effects," International Journal of Heat and Mass Transfer, vol. 139, pp. 713–719, 2019.
24. H. Sardar, L. Ahmad, M. Khan, and A. S. Alshomrani, "Investigation of mixed convection flow of Carreau nanofluid over a wedge in the presence of Soret and Dufour effects," International Journal of Heat and Mass Transfer, vol. 137, pp. 809–822, 2019.

25. M. Bilal Ashraf, T. Hayat, S. A. Shehzad, and B. Ahmed,“Thermophoresis and MHD mixed convection three-dimensional flow of viscoelastic fluid with Soret and Dufour effects,” Neural Computing & Applications, vol. 31, no. 1, pp. 249–261, 2019.
26. N. Jiang, E. Studer, and B. Podvin, “Physical modeling of simultaneous heat and mass transfer: species interdiffusion, Soret effect and Dufour effect,” International Journal of Heat and Mass Transfer, vol. 156, Article ID 119758, 2020.
27. A. Hafeez, M. Khan, and J. Ahmed, “Oldroyd-B fluid flow over a rotating disk subject to Soret–Dufour effects and thermophoresis particle deposition,” Proceedings of the Institution of Mechanical Engineers - Part C: Journal of Mechanical Engineering Science, vol. 235, no. 13, Article ID 0954406220946075, 2020.
28. M. K. Nayak, “MHD 3D flow and heat transfer analysis of nanofluid by shrinking surface inspired by thermal radiation and viscous dissipation,” International Journal of Mechanical Sciences, vol. 124-125, pp. 185–193, 2017.
29. B. Ramandevi, J. V. R. Reddy, V. Sugunamma, and N. Sandeep, “Combined influence of viscous dissipation and non-uniform heat source/sink on MHD non-Newtonian fluid flow with Cattaneo-Christov heat flux,” Alexandria Engineering Journal, vol. 57, no. 2, pp. 1009–1018, 2018.
30. U. Farooq, D. Lu, S. Munir, M. Ramzan, M. Suleman, and S. Hussain, “MHD flow of Maxwell fluid with nanomaterials due to an exponentially stretching surface,” Scientific Reports, vol. 9, no. 1, pp. 7312–7411, 2019.
31. B. Mahanthesh, B. J. Gireesha, I. L. Animasaun, T. Muhammad, and N. S. Shashikumar, “MHD flow of SWCNT and MWCNT nanoliquids past a rotating stretchable disk with thermal and exponential space dependent heat source,” Physica Scripta, vol. 94, no. 8, Article ID 085214, 2019.
32. H. R. Patel and R. Singh, “.ermophoresis, Brownian motion and non-linear thermal radiation effects on mixed convection MHD micropolar fluid flow due to nonlinear stretched sheet in porous medium with viscous dissipation, joule heating and convective boundary condition,” International Communications in Heat and Mass Transfer, vol. 107, pp. 68–92, 2019.
33. E. H. Aly and I. Pop, “MHD flow and heat transfer over a permeable stretching/shrinking sheet in a hybrid nanofluid with a convective boundary condition,” International Journal of Numerical Methods for Heat and Fluid Flow, 2019.
34. I. Rashid, M. Sagheer, and S. Hussain, “Entropy formation analysis of MHD boundary layer flow of nanofluid over a porous shrinking wall,” Physica A: Statistical Mechanics and Its Applications, vol. 536, Article ID 122608, 2019.
35. I. Waini, A. Ishak, and I. Pop, “MHD flow and heat transfer of a hybrid nanofluid past a permeable stretching/shrinking wedge,” Applied Mathematics and Mechanics, vol. 41, no. 3, pp. 507–520, 2020.
36. Sheikhpour M, Arabi M, Kasaeian A, et al. Role of nanofluids in drug delivery and biomedical technology: Methods and applications. Nanotechnol Sci Appl. 2020;13:47.

37. Khanafer, K., Vafai, K. Applications of nanofluids in porous medium. J Therm Anal Calorim. 2019;135(2):1479-1492.
38. Wang XQ, Mujumdar AS. A review on nanofluids-part II: experiments and applications. Braz J Chem Eng. 2008;25:631-648.
39. Haroon U. R. Rasheed, Saeed Islam, Zeeshan Khan, Sayer O. Alharbi, Hammad Alotaibi, Ilyas Khan, "Impact of Nanofluid Flow over an Elongated Moving Surface with a Uniform Hydromagnetic Field and Nonlinear Heat Reservoir", Complexity, vol. 2021, Article ID 9951162, 9 pages, 2021. https://doi.org/10.1155/2021/9951162
40. Islam, S.; Ur Rasheed, H.; Nisar, K.S.; Alshehri, N.A.; Zakarya, M. Numerical Simulation of Heat Mass Transfer Effects on MHD Flow of Williamson Nanofluid by a Stretching Surface with Thermal Conductivity and Variable Thickness. Coatings 2021, 11, 684. https://doi.org/10.3390/coatings11060684
41. Zeeshan, Rasheed, H.U., Khan, W. et al. Numerical computation of 3D Brownian motion of thin film nanofluid flow of convective heat transfer over a stretchable rotating surface. Sci Rep 12, 2708 (2022). https://doi.org/10.1038/s41598-022-06622-9
42. Khan, Z.; Rasheed, H.U.; Khan, I.; Abu-Zinadah, H.; Aldahlan, M.A. Mathematical Simulation of Casson MHD Flow through a Permeable Moving Wedge with Nonlinear Chemical Reaction and Nonlinear Thermal Radiation. Materials 2022, 15, 747. https://doi.org/10.3390/ma15030747.